

## Smectic ordering of octylcyanobiphenyl confined to control porous glasses

This article has been downloaded from IOPscience. Please scroll down to see the full text article.

2000 J. Phys.: Condens. Matter 12 A431

(<http://iopscience.iop.org/0953-8984/12/8A/359>)

View [the table of contents for this issue](#), or go to the [journal homepage](#) for more

Download details:

IP Address: 129.252.86.83

The article was downloaded on 27/05/2010 at 11:28

Please note that [terms and conditions apply](#).

## Smectic ordering of octylcyanobiphenyl confined to control porous glasses

A Zidanšek†, S Kralj†‡, R Repnik‡, G Lahajnar†, M Rappolt§, H Amenitsch§ and S Bernstorff||

† J Stefan Institute, Jamova 39, 1000 Ljubljana, Slovenia

‡ Faculty of Education, University of Maribor, Koroška 160, 2000 Maribor, Slovenia

§ Institute of Biophysics and X-ray Structure Research, Austrian Academy of Sciences, Graz, Austria

|| ELETTRA, Sincrotrone Trieste, AREA Science Park, Trieste, Italy

Received 12 August 1999

**Abstract.** We performed an x-ray scattering study of the smectic A (SmA) ordering of the liquid crystal 8CB (octylcyanobiphenyl) confined to a control porous glass with a typical void radius  $R = 0.2 \mu\text{m}$ . The voids were either nontreated or covered with silane. The results reveal a strong influence of spatial restriction and surface treatment on the temperature evolution of smectic ordering. The observations are qualitatively reproduced using the Landau–Ginsburg approach.

### 1. Introduction

For years there has been a steady interest in the physics of liquid crystals confined to various porous matrices [1]. As confined matrices aerogels [2–5], Russian glasses [6, 7], Vycor glasses [8, 9], control porous glasses (CPGs) [10–13] and Anopore [14] or Nuclepore [15] are most commonly used. Such systems exhibit a rich variety of different physical phenomena interesting both for understanding fundamental principles of physics as well as for various applications. In particular, phenomena related to finite size effects, surface interactions (wetting, anchoring) and randomness could be manifested in these systems.

In this contribution we study octylcyanobiphenyl (8CB) liquid crystals (LCs) confined to control porous glass matrices focusing on the nematic–SmA phase transition. The smectic ordering is probed using small angle x-ray scattering (SAXS). A CPG matrix consists of cylindrically shaped voids that are strongly curved and interconnected. The curvature and interconnectedness are rather randomly distributed introducing some kind of randomness into the system. The pore diameter distribution is monodispersed with a 5–10% variation in size. The surface of the voids is smooth down to the nm scale. The phase and the structure of confined liquid crystal in these systems reflect the interplay between elastic and surface interactions where finite size effects and randomness can play a significant role.

The plan of the paper is the following. In section 2 we present experimental results. The theoretical model is given in section 3. The results are discussed in section 4 and summarized in the last section.

## 2. Experiment

We used CPG matrices with monodispersed radius  $R = (200 \pm 20)$  nm of cylindrically shaped voids. The voids' surface was either nontreated or silane-treated. Henceforth we refer to these samples as nontreated and treated respectively. Based on previous studies [10–13] on CPG samples we assume that the easy axis (if an LC molecule orients along this orientation it minimizes orientational surface anchoring free energy) is lying in the plane (tangential orientational anchoring) for the nontreated surface and along the surface normal (homeotropic orientational anchoring) in the silane-treated case.

The SAXS patterns were measured between 20 and 50 °C. A first order diffraction peak was observed at the inverse distance between the smectic layers in the smectic A phase. From the amplitude of the peak the average degree of smectic ordering is determined. The lineshape is fitted to a Lorentzian, where the linewidth reveals the smectic correlation length  $\xi$  for the confined liquid crystal.

In figure 1 we show the temperature evolution of the smectic ordering across the bulk nematic–SmA phase transition for the bulk, silane-treated and nontreated sample.

## 3. Theory

We describe LC ordering in terms of the nematic director field  $\bar{n}$  and the complex smectic order parameter  $\psi = \eta e^{i\phi}$ . Here  $\bar{n}$  points along the local average orientation of a rodlike liquid crystal molecule,  $\eta$  is the translational smectic order parameter and the phase  $\phi$  determines the position of smectic layers. In terms of these continuum fields the free energy of the confined LC phase is expressed as

$$F = \iiint (f_e^{(n)} + f_h^{(s)} + f_e^{(s)}) d^3\bar{r} + \iint (f_a^{(n)} + f_a^{(s)}) d^2\bar{r}. \quad (1)$$

Here  $f_i^{(phase)}$  stand for free energy densities. The superscript (*phase*) determines either nematic (*n*) or smectic (*s*) contribution. The subscript *i* determines bulk elastic (*e*), bulk homogeneous (*h*) or surface anchoring interaction (*a*) term. We write free energy densities as [16–18]

$$f_h^{(s)} = a_0 \frac{T - T_{NA}}{T_{NA}} |\psi|^2 + \frac{b}{2} |\psi|^4 \quad (2a)$$

$$f_e^{(n)} = \frac{K}{2} ((\nabla \cdot \bar{n})^2 + (\nabla \times \bar{n})^2) \quad (2b)$$

$$f_e^{(s)} = C (|\bar{n} \cdot \nabla - iq_0 \psi|^2 + |\bar{n} \times \nabla \psi|^2) \quad (2c)$$

$$f_a^{(n)} = \frac{W^{(n)}}{2} (1 - (\bar{e}_s \cdot \bar{n})^2) \quad (2d)$$

$$f_a^{(s)} = \frac{W^{(s)}}{2} |\psi - \psi_s|^2. \quad (2e)$$

The quantities  $a_0$ ,  $b$  are the material constants,  $T$  is the temperature,  $T_{NA}$  the temperature of the second order N–SmA phase transition. In the unconstrained SmA phase the bulk smectic order parameter is given by  $\eta_b = \sqrt{a_0(T_{NA} - T)/bT_{NA}} = \eta_0 \sqrt{-\tau}$ . Here  $\eta_0$  stands for the ‘saturated’ degree of smectic ordering deep in the SmA phase and  $\tau = (T - T_{NA})/T_{NA}$  is the reduced temperature. The elastic terms are expressed in a single elastic constant approximation in terms of the effective nematic ( $K$ ) and smectic ( $C$ ) elastic constant. The smectic elastic terms enforce layer periodicity  $q_0$ . The nematic and smectic anchoring potential, expressed in the lowest order approximation (expansion in the relevant order parameter), are weighted

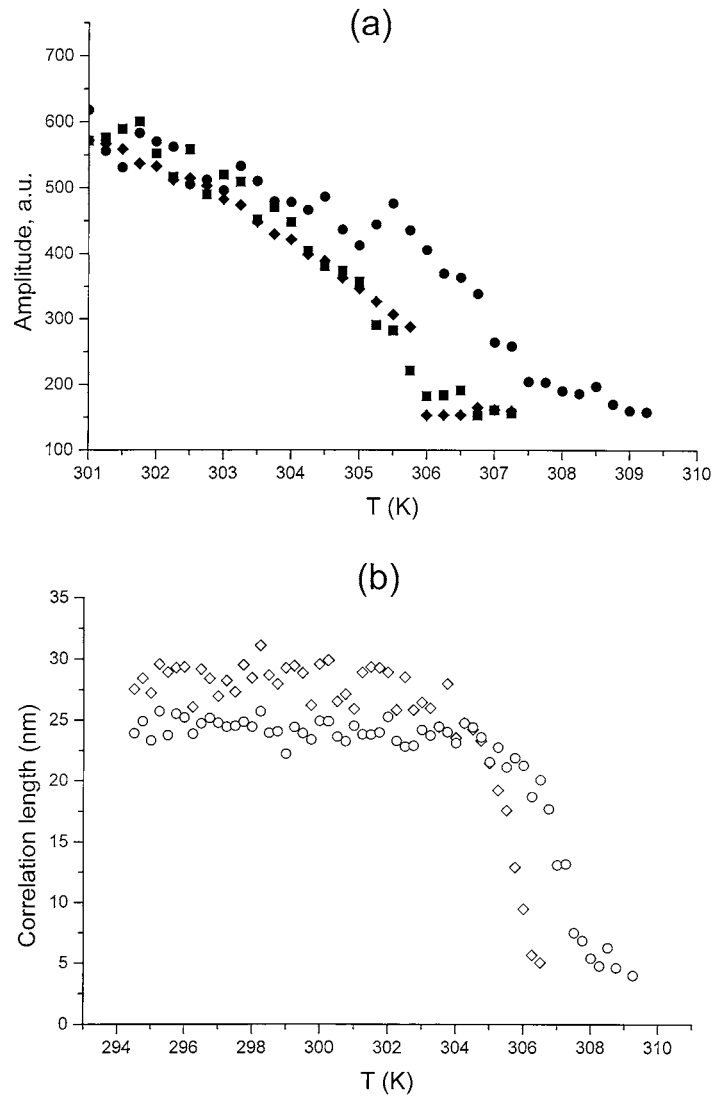


**Figure 1.** Temperature evolution of smectic ordering. (a)  $\eta = \eta(T)$ , (b)  $\xi = \xi(T)$ . Circles: treated sample; diamonds: nontreated sample; squares: bulk.

with constants  $W^{(s)}$  and  $W^{(n)}$  respectively. The nematic orientational anchoring tends to orient LC molecules along the easy axis  $\vec{e}_s$  and the smectic positional anchoring tends to establish smectic ordering  $\psi_s$  preferred by the surface.

#### 4. Discussion

In bulk the N–SmA phase transition is continuous. Consequently the bulk smectic correlation length  $\xi_b$  is expected to diverge at  $T = T_{NA}$ . Above  $T_{NA}$  the model yields  $\xi_b = \sqrt{C/a_0(T - T_{NA})/T_{NA}} = \xi_0/\tau$ , where  $\xi_0$  stands for the ‘bare’ smectic correlation length. The measured temperature dependence  $\xi = \xi(T)$  displays distinctively different behaviour

as evident from figure 1(b). In both treated and nontreated samples the correlation lengths monotonically increase with decreasing temperature approaching roughly the typical linear void size  $R$ .

In order to qualitatively reproduce this observation we assume that, approaching the bulk N–SmA phase transition with decreasing temperature, domains with smectic ordering form, of typical linear size  $\xi_d$ . Each smectic domain is surrounded either by nematic phase (with director field incompatible with smectic ordering) or cavity wall. The ‘incompatible’ smectic areas are a consequence of randomly connected cavities and random curvatures that may locally enforce strong elastic distortions in the smectic ordering. A sample thus exhibits a polydomain structure. For simplicity we further assume that within a domain molecules are aligned in a single orientation along which smectic ordering exhibits spatial variation. In general within a domain the phase differs from its equilibrium value. To minimize the imposed layer stress the phase exhibits spatial variation over the available size which is in this case given by  $\xi_d$  (the bulk Euler–Lagrange equation for  $\phi$  does not explicitly contain any typical length except the domain size [19]). Therefore the smectic elastic contribution  $\eta^2(\bar{n} \cdot \nabla\phi - q_0)^2$  is roughly given by  $(\eta\delta\phi/\xi_d)^2$  where  $\delta\phi$  describes departures from the equilibrium phase over distance  $\xi_d$ . Consequently within the cavity one obtains

$$f_h^{(s)} + f_e^{(s)} \approx \eta^2 \left( a_0 \frac{T - T_{NA}}{T_{NA}} + C \left( \frac{\delta\phi}{\xi_d} \right)^2 \right) + \frac{b}{2} \eta^4$$

yielding the following expression for the smectic translational order parameter correlation length of the confined LC:

$$\xi = \sqrt{\frac{C}{a_0(T - T_{NA})/T_{NA} + C(\delta\phi/\xi_d)^2}} \quad (3)$$

In the case where the contribution including  $\xi_d$  is dominant (i.e. small domains) one obtains  $\xi \approx \xi_d/\delta\phi$ . With decreased temperature the domain size increases (and thus also  $\xi_d$ ) saturating below the typical linear cavity size  $R$ .

We next focus on the temperature dependence of the smectic order parameter. In particular the treated sample, in which the surface enforces homeotropic anchoring, exhibits qualitatively different behaviour compared to the bulk sample. The results suggest that there exists some residual smectic ordering also above  $T_{NA}$ . This is expected if the anchoring is strong enough to enforce the homeotropic anchoring requiring [16]  $W^{(n)}R/K > 1$ . For  $R = 0.2 \mu\text{m}$  and  $K \approx 10^{11} \text{ N}$  one obtains  $W^{(n)} > 2.5 \times 10^{-5} \text{ J m}^{-2}$ , which is reasonable for silane coating. In this case the coupling between the surface and smectic ordering is relatively strong because the first smectic layer is all in contact with the surface. The ordering tendencies of the surface are similar to an effectively lower temperature promoting smectic ordering. As expected this prewetting mechanism is not observed in the nontreated sample where coupling between the substrate and smectic layers is much weaker.

In order to demonstrate this qualitatively using our model we consider a plane-parallel cell whose wall enforces homeotropic anchoring and supports smectic ordering (i.e.  $W^{(s)} > 0$ ). For simplicity we assume that (i)  $\eta$  is allowed to vary only along the normal of plates which is set along the  $x$ -axis of the Cartesian co-ordinate system, (ii)  $\bar{n} = (1, 0, 0)$  is homogeneously aligned along the  $x$ -axis and (iii) the layers have bulk equilibrium spacing ( $\phi = q_0x$ ). The cell plates are set at  $x = 0$  and  $x = R$ .

For numerical purposes we introduce the scaled quantities  $\tilde{x} = x/R$ ,  $\tilde{\eta} = \eta/\eta_0$  and introduce the smectic surface extrapolation length  $d_e^{(s)} = W_a^{(s)}\eta_0/C\eta_0^2$ . We subsequently drop

the tildes. With this in mind one obtains for the dimensionless free energy  $G$ :

$$G = \int_0^1 \left( \left( \frac{R}{\xi_0} \right)^2 \left( \tau \eta^2 + \frac{\eta^4}{2} \right) + \left( \frac{d\eta}{dx} \right)^2 \right) dx - \frac{R}{d_e^{(s)}} \eta(x=0) - \frac{R}{d_e^{(s)}} \eta(x=1). \quad (4)$$

We obtain  $\eta = \eta(x)$  via minimization of equation (4). The dependence  $\eta = \eta(x)$  exhibits residual smectic ordering also at  $T > T_{NA}$  for strong enough positional anchoring ( $R/d_e^{(s)} > 1$ ). In figure 2 we plot the average smectic order parameter  $\eta_a = \int_0^1 \eta(x) dx$  as a function of temperature. One sees that presmectic ordering is clearly visible.

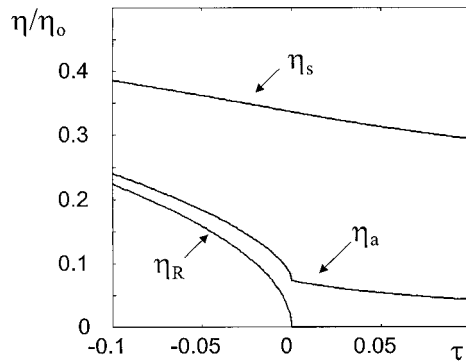


**Figure 2.** Simulated temperature evolution of smectic ordering.  $\eta_s$ : degree of smectic ordering at the surface;  $\eta_R$ : smectic ordering in the centre of the cell.  $R/d_e^{(s)} = 10$ ,  $(R/\xi_0)^2 = 1000$ .

## 5. Conclusions

We investigated the phase behaviour of 8CB LC confined into CPG matrices focusing on the N–SmA phase transition. The voids' wall was either nontreated or silane-treated. Consequently the orientational anchoring is expected to be tangential and homeotropic, respectively. The voids' radii are large enough ( $R = 0.2 \mu\text{m}$ ) so that the orientational anchoring tendency is actually realized.

The temperature evolution of smectic ordering reveals a dramatic influence on confinement and surface treatment in comparison to the bulk behaviour. In both samples (treated and nontreated) the correlation length monotonically increases with decreasing temperature saturating below  $R$ . We attribute such behaviour to a smectic domain structure where the typical domain size monotonically increases with decreasing  $T$ . Smectic domains are in this picture visualized as smectic islands surrounded by the nematic phase or cavity wall. The domain structure results from the randomness introduced via random curvature of voids and random interconnections among different voids.

In the treated sample presmectic behaviour is observed. In this case the coupling interaction between the surface and LC is strong enough to cover the voids' surface with a few smectic layers above the bulk nematic–SmA phase transition. In the nontreated sample this behaviour is not observed. Theoretical considerations suggest that pretransitional smectic wetting is realized if  $R/d_e^{(s)} < 1$ .

**References**

- [1] Crawford G P and Žumer S (eds) 1996 *Liquid Crystals in Complex Geometries formed by Polymer and Porous Networks* (London: Taylor and Francis)
- [2] Clark N A, Bellini T, Malzbender R M, Thomas B N, Rappaport A G, Muzny C D, Schaefer D W and Hrubesh L 1993 *Phys. Rev. Lett.* **71** 3505
- [3] Schwalb G and Deeg F W 1995 *Phys. Rev. Lett.* **74** 1383
- [4] Zidanšek A, Kralj S, Lahajnar G and Blinc R 1995 *Phys. Rev. E* **51** 3332
- [5] Mertelj A and Čopič M 1997 *Phys. Rev. E* **55** 504
- [6] Aliev F M 1988 *Kristallografiya* **33** 969 (Engl. transl. 1988 *Sov. Phys.–Crystallogr.* **33** 573)
- [7] Aliev F M and Breganov M N 1989 *Zh. Eksp. Teor. Fiz.* **95** 122 (Engl. transl. 1989 *Sov. Phys.–JETP* **68** 70)
- [8] Iannacchione G S, Crawford G P, Žumer S, Doane J W and Finotello D 1993 *Phys. Rev. Lett.* **71** 2595
- [9] Tripathy S, Rosenblatt C and Aliev F M 1994 *Phys. Rev. Lett.* **72** 2725
- [10] Dadmun M D and Muthukumar M 1993 *J. Chem. Phys.* **98** 4850
- [11] Kralj S, Zidanšek A, Lahajnar G, Mušević I, Žumer S, Blinc R and Pintar M M 1996 *Phys. Rev. E* **53** 3629
- [12] Cramer Ch, Cramer Th, Kremer F and Stannarius R 1997 *J. Chem. Phys.* **106** 3730
- [13] Kralj S, Zidanšek A, Lahajnar G, Žumer S and Blinc R 1998 *Phys. Rev. E* **57** 3021
- [14] Iannacchione S, Mang J T, Kumar S and Finotello D 1994 *Phys. Rev. Lett.* **73** 2708
- [15] Crawford R O, Crawford G P, Doane J W, Žumer S, Vilfan M and Vilfan I 1993 *Phys. Rev. E* **48** 1998
- [16] de Gennes P G and Prost J 1993 *The Physics of Liquid Crystals* (Oxford: Oxford University Press)
- [17] Renn S R and Lubensky T C 1988 *Phys. Rev. A* **38** 2132
- [18] Slavinec M, Kralj S, Žumer S and Sluckin T J *Phys. Rev. Lett.* submitted
- [19] Kralj S, Pirš J, Žumer S and Petkovšek R 1998 *J. Appl. Phys.* **84**